Inorganic Chemistry
Cite This: Inorg. Chem. 2018, 57, 6913−6920
Article
pubs.acs.org/IC

Determination of d-Orbital Populations in a Cobalt(II) Single-Molecule Magnet Using Single-Crystal X-ray Diffraction

Matthew Craven,[†] Mathilde H. Nygaard,[†] Joseph M. Zadrozny,[‡,⊥] Jeffrey R. Long,[‡,§,∥] and Jacob Overgaard*[,†]

[†]Department of Chemistry, Aarhus University, Langelandsgade 140, DK-8000 Aarhus C, Denmark
[‡]Department of Chemistry and [§]Department of Chemical and Biomolecular Engineering, University of California, Berkeley, California 94720, United States
[∥]Materials Sciences Division, Lawrence Berkeley National Laboratory, Berkeley, California 94720, United States

Supporting Information

ABSTRACT: The tetrahedral cobalt(II) compound $(Ph_4P)_2[Co(SPh)_4]$ was the first mononuclear transition-metal complex shown to exhibit slow relaxation of the magnetization in zero external magnetic field. Because the relative populations of the d orbitals play a vital role in dictating the magnitude of the magnetic anisotropy, the magnetic behavior of this complex is directly related to its electronic structure, yet the exact role of the soft, thiophenolate ligands in influencing the d-electron configuration has previously only been investigated via theoretical methods. To provide detailed experimental insight into the effect of this ligand field, the electron density distribution in this compound was determined from low-temperature, single-crystal X-ray diffraction data and subsequent multipole modeling. Topological analysis of the electron density indicates significant covalent contributions to the cobalt−sulfur bonds. The derived d-orbital populations further reveal a fully occupied d_{z^2} orbital, minor d_{xz} orbital population, and nearly equal population of the d_{xy}, $d_{x^2-y^2}$, and d_{yz} orbitals. Notably, we find that an electrostatic interaction between Co(II) and one hydrogen atom from a thiophenolate group in the *xz* plane increases the energy of the $d_{x^2-y^2}$ orbital, leading to the nearly equal population with d_{xy} and strong magnetic anisotropy.

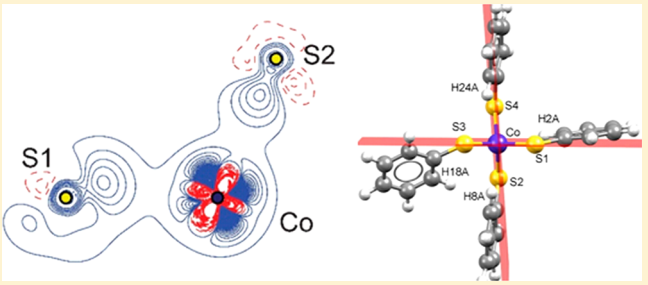

INTRODUCTION

Molecular magnetism is continuously evolving, as new compounds with exciting magnetic properties are realized. The quest for single-molecule magnets is particularly intriguing, as they are potentially useful as the individual bits in memory storage devices or as components in quantum computers.[1,2] Since the early 1990s and the discovery of molecule-based magnetic hysteresis in the cluster $Mn_{12}O_{12}(CH_3COO)_{16}(H_2O)_4$,[3] many other polynuclear transition-metal compounds[4] and mononuclear lanthanide[5] systems have been shown to exhibit slow magnetic relaxation, yet the complex magnetic behavior exhibited by these compounds renders the interpretation of their properties a challenge. Structurally and electronically simpler compounds are desirable toward simplified analysis and enhanced fundamental insight, and therefore mononuclear transition-metal-based single-molecule magnets have garnered increased interest.[6−10] The first zero-field single-molecule magnet in this class was the tetraphenylphosphonium salt of the tetrahedral complex $[Co(SPh)_4]^{2-}$, which was revealed via alternating current (ac) magnetic susceptibility measurements to have an energy barrier to spin reversal of $U_{eff} = 21(1)$ cm^{-1}.[11] The magnetic anisotropy in this complex originates from orbital angular momentum generated from mixing of the excited state into the ground state via spin−orbit coupling, which is a second-order effect that can be expressed quantitatively using the zero-field splitting parameter *D*. The Se analogue of this compound, $(Ph_4P)_2[Co(SePh)_4]$, was later identified to exhibit slow magnetic relaxation arising from the same phenomenon.[12] Diffuse reflectance spectroscopic data collected on powder samples of $[Co(EPh)_4]^{2-}$ (E = O, S, Se) were used to derive d-orbital energy splittings, indicating the ($d_{x^2-y^2}$, d_{xy}) orbitals are lower in energy than (d_{xz}, d_{yz}), with d_{z^2} significantly lower than both sets, and with a total d-orbital splitting of less than 8000 cm^{-1} in each compound that decreased with increasing soft character of the ligand. Because the absolute value of *D* is inversely proportional to the energy separation between the two (sets of) orbitals that are unevenly populated, softer ligands are expected to lead to larger anisotropy and therefore larger |*D*|. These concepts have been discussed on theoretical and experimental grounds in several recent publications.[13,14]

Despite the comprehensive nature of the foregoing studies, there are still remaining questions about the true role of ligand

Received: February 28, 2018
Published: June 4, 2018

Downloaded via UNIV OF CALIFORNIA BERKELEY on June 20, 2018 at 17:23:03 (UTC).
See https://pubs.acs.org/sharingguidelines for options on how to legitimately share published articles.

© 2018 American Chemical Society

DOI: 10.1021/acs.inorgchem.8b00513
Inorg. Chem. 2018, 57, 6913−6920

covalency on the magnetic properties of the $[Co(EPh)_4]^{2-}$ complexes. For example, as highlighted in ref 12, the lowest-energy absorption between the $d_{x^2-y^2}$ and d_{xy} orbitals is small (~1000 cm^{-1}) and therefore not readily detectable via optical spectroscopy. Consequently, the relative energies of these two orbitals have not been precisely determined, and the true contribution of the $(d_{x^2-y^2}, d_{xy})^3$ electronic configuration to the anisotropy is unknown. It was also noted in the same work[12] that a higher extent of covalency in the metal−ligand bonding may lead to an increase in the magnetic anisotropy (and an enhancement of the magnetic properties), because the heavier ligand analogue has a larger spin−orbit coupling parameter. This approach of using heavy ligands to enhance magnetic anisotropy has more recently been explored in the study of Fe^{2+} compounds bearing both group 14 and halide ligands, where it was identified that beyond simply seeking enhanced covalent interactions, targeting enhanced covalency between spin-bearing molecular orbitals is key to influencing magnetic anisotropy.[15] Because information about both the nature of the bonding and the d-orbital splitting is not directly available from spectroscopic[16−19] or magnetic measurements, as presented in previous studies,[11,12] new measurements and interpretations are necessary to obtain a broader understanding of anisotropy in $[Co(SPh)_4]^{2-}$.

In contrast to the existing studies on $[Co(SPh)_4]^{2-}$, analysis of electron density, obtained experimentally from single-crystal X-ray diffraction,[20−24] can provide a thorough description of the nature of the chemical bonding[25,26] as well as an estimate of the d-orbital populations.[27] Although d-orbital energies are not strictly accessible from the electron density, it is possible to obtain quantitative estimation of their relative populations and thus an indirect measure for their relative energies. A topological analysis of the electron density $\rho(r)$, moreover, leads to the location of so-called bond critical points (bcp) between all bonded atoms, and the evaluation of the electron density at these points ($\rho_{bcp}(r)$) and of the second derivative of the electron density, called the Laplacian, $\nabla^2\rho_{bcp}(r)$, provides important information about the nature of the bonding.[26,28,29] In particular, when inspecting bonding between second-row elements, the sign of the Laplacian unambiguously classifies the bonds as either covalent ($\nabla^2\rho_{bcp}(r) < 0$) or ionic ($\nabla^2\rho_{bcp}(r) > 0$). However, such a strict and dichotomous classification scheme becomes muddled when heavier elements are involved and/or when the electronegativity difference between the two constituent atoms is large. Alternatively, the nature of the bonding can be described using the total energy density H, which is also accessible from the electron density[30,31] and is simply the sum of the potential (V, always negative) and kinetic (G, always positive) energy densities, where the former reflects covalency and the latter ionicity. Given the wealth of information accessible from electron density analysis, we sought to investigate in detail the chemical bonding within $(Ph_4P)_2[Co(SPh)_4]$ using this technique, with the goal of deriving fundamental insight into the electronic structure of the cobalt(II) center.

Herein, we use electron density to extract the energetic ordering and occupancy of the d-orbitals and the distribution of charges, and to quantitate the covalent nature of the Co−S bonds in $[Co(SPh)_4]^{2-}$, providing important and previously lacking experimental corroboration of the current view of the electronic structure of this complex. Notably, we also find from these data that the positioning of select hydrogen atoms near the central Co plays a key role in determining the magnetic anisotropy of the complex.

EXPERIMENTAL METHODS

General Methods. The compound $(Ph_4P)_2[Co(SPh)_4]$ was synthesized according to a previously reported procedure.[11] All reagents were purchased from commercial suppliers and used as received.

Single-Crystal X-ray Diffraction. Single-crystal diffraction data were collected on an Oxford Diffraction Supernova diffractometer using a microfocus Mo Kα tube (λ = 0.710 73 Å). A single crystal with the desired dimensions (~200 μm in all directions) was selected and mounted on a goniometer head using mineral oil. The crystal was cooled to 100 K using a Cryosystems Cryostream 700 device prior to data collection. The program CrysalisPro[32] was used to control the data collection and for the subsequent data reduction. A total of 267 745 reflections were corrected for absorption effects using a Gaussian approach based on indexed crystal faces. Equivalent reflections were merged with SORTAV,[33] and only reflections measured more than once were selected to provide a total of 37 498 unique reflections with an internal agreement of R_{int} = 0.057. The crystal structure was solved using the direct methods program SHELXT[34] and refined using SHELXL[35] in Olex2.[36] An ORTEP[37] depiction of the molecular structure of the $[Co(SPh)_4]^{2-}$ complex is shown in Figure 1.

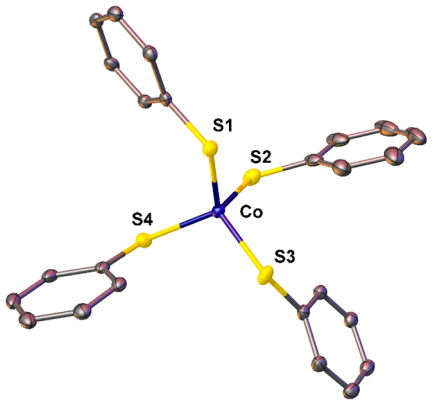

Figure 1. ORTEP drawing of the structure of the $[Co(SPh)_4]^{2-}$ complex, as determined by X-ray diffraction analysis of a single crystal of $(Ph_4P)_2[Co(SPh)_4]$, showing 50% probability ellipsoids. A drawing of the full asymmetric unit can be found in the Supporting Information.

Multipole Modeling. The aspherical electron density distribution in $(Ph_4P)_2[Co(SPh)_4]$ was modeled using a pseudoatom multipolar description, as described by Hansen et al.,[38] using the XD program package.[39] The multipole model redefines the atomic electron density using eq 1, separating it into core, spherical valence, and aspherical valence parts:

$$\rho_{atom} = P_c\rho_c(r) + P_v\rho_v\kappa^3(\kappa\mathbf{r}) + \sum_{l=0}^{l_{max}}\kappa'^3 R_l(r)\sum_{m=0}^{l} P_{lm\pm}d_{lm\pm}(\theta, \varphi) \quad (1)$$

In eq 1, the κ and κ' parameters describe modified radial behavior of the density functions belonging to the spherical and aspherical valence parts, respectively, such that when $\kappa < 1$ the shell is expanded relative to the calculated gas-phase atomic reference density. The angular redistribution of electron density is described by the d_{lm} functions, which are hydrogenic orbitals with slightly different normalization constants. A multipolar model consists of refining the population parameters P_{lm} against the experimental structure factors. After an initial refinement of scale factors, a high-order independent atom model (IAM) refinement was performed using only reflections with

DOI: 10.1021/acs.inorgchem.8b00513
Inorg. Chem. 2018, 57, 6913−6920

$\sin(\theta)/\lambda$ values above 0.7 Å^{-1}. This refinement included only positional and anisotropic thermal parameters for non-H atoms. All C−H bond distances were fixed to 1.09 Å.[40] After this, the C−H bond length constraint was temporarily lifted, and hydrogen positional and isotropic thermal parameters were refined using only reflections with $\sin(\theta)/\lambda$ values below 0.7 Å^{-1}. These refinements laid a structural foundation for the forthcoming refinements. An ionic scattering factor for Co^{2+} was used,[41] while the remaining atoms were described using neutral scattering factors.[42] The overall charges for the two $(Ph_4P)^{n+}$ cations and the anionic $[Co(SPh)_4]^{m-}$ complex were fixed to n = 1, 1 and m = 2 from the sum of the valence population parameters, and these values were maintained throughout subsequent refinements to ensure overall charge neutrality.

Subsequently we performed refinement of all κ values along with monopole population parameters. Multipole population parameters were then refined stepwise, up to hexadecapoles for Co, S, and P (l_{max} = 4) and octupoles for C (l_{max} = 3). Hydrogen atoms were refined with one monopole and a single dipole along the bond direction. Refinement of κ' was attempted but was found to give unrealistic values for Co and S, and so this parameter was only refined for P and C, while for Co and S the values were fixed to unity. Symmetry restrictions were removed for Co and S, and all multipole functions were refined up to l = 4. This refinement included 1982 parameters. Finally, all positional and thermal parameters were refined for non-H atoms.

A pattern of residual density characteristic of unmodelled anharmonic thermal motion[43] was found around the sulfur atoms and atom S2, in particular. This residual density could be substantially reduced by inclusion of anharmonic thermal parameters for S2. The associated probability density was everywhere positive and thus physically sensible. In addition to the sign of anharmonicity in the atomic vibrations, the final analysis revealed a localized region of large residual density distant (>2 Å) from all other atoms and closest to a hydrogen atom. We ascribed this residual density to a peculiar result of the presence of random errors in the data, as there is minimal possibility for any atom (even partially occupied) to be present at this position. Examination of the thermal parameters from the final model showed that all bonds are rigid, fulfilling Hirshfeld's rigid bond test,[44] with the average difference of mean-square displacement amplitudes equal to 6.4 × 10^{-4} Å^2. An analysis of the residual density distribution using the fractal dimensionality approach of Henn and Meindl[45,46] was performed to quantify the featurelessness of the data. This analysis clearly showed that the remaining residuals can be ascribed to random errors in the data (see Figure S1); as mentioned above, the largest residual density (0.44 e Å^{-3}) is located in a region far from any atom and is therefore not a sign of unmodelled disorder, although it does bias the parabola toward positive values. Table 1 outlines the pertinent crystallographic details, while more details can be found in the Supporting Information.

RESULTS

No significant differences were found between the crystal structure of $[Co(SPh)_4]^{2-}$ published in ref 11 and the structure presented here, and we note that, as found previously, the geometry around the cobalt(II) center exhibits a large distortion from idealized tetrahedral coordination, with S−Co−S angles that range from 96.6(1)° to 119.9(1)° (Table 2). Even still, the $[Co(SPh)_4]^{2-}$ moiety can be approximated as a tetrahedron (the continuous shape measure calculated using SHAPE software[47] is 1.15), and to some extent the phenyl rings lie within the two nearly perpendicular planes formed by S1−Co−S3 and S2−Co−S4, with only the phenyl ring attached to S3 significantly distorted out of its respective plane (Figure 2). This distortion results from the combined rotation around the S−C bonds, giving torsion angles (C−C−S−Co) of −2.5°, 4.1°, 27.4°, and −18.5° for S1 to S4, respectively, and a rotation around the Co−S3 bond. The effect is that the hydrogen atom (H18A) on the C_α atom of the phenyl ring on S3, which is exposed to Co, is moved further away from Co ($d_{Co\cdots H}$ = 3.11 Å) compared to the similar H atoms on the other three rings (where the Co···H distances range from 2.68 to 2.84 Å). However, in this position, H18A is also placed directly between the Co−S bonds when viewed as in Figure 2b. This positioning is of relevance for the interpretation of the d-orbital populations below.

An extensive range of intermolecular interactions occur between the sulfur atoms and the phenyl rings, both of the C−H···S type as well as several intra- and intermolecular $\pi\cdots\pi$ interactions. The sum of these weak interactions contributes to the cohesive energy of the crystal structure, but considering the charged nature of the constituent ions, the electrostatic energy is likely a more important factor dictating the lattice energy. The abundance of intermolecular interactions is found only between two neighboring phosphonium ions or between a $[Co(SPh)_4]^{2-}$ complex and a phosphonium ion. The nearest Co···Co distance is on the order of 10 Å, and previous magnetic characterization of a sample of $[Co(SPh)_4]^{2-}$ diluted within a matrix of isostructural, diamagnetic $[Zn(SPh)_4]^{2-}$ complexes revealed no change in the static magnetic behavior. Given the absence of any pathways for strong magnetic communication between Co sites, we do not discuss intermolecular interactions further.

Experimental electron density analyses of single-crystal structural data can provide a complete analytical description of the electronic accumulation and depletion that occurs at a

Table 1. Crystallographic Parameters

	$(Ph_4P)_2[Co(SPh)_4]$
formula	$C_{72}H_{60}CoP_2S_4$
weight, g mol^{-1}	1174.31
crystal system	orthorhombic
space group	$Pca2_1$
Z	4
a, Å	17.4010(2)
b, Å	13.6160(1)
c, Å	24.6260(3)
V, Å^3	5834.7(1)
T, K	100
ρ, g cm^{-3}	1.336
μ, mm^{-1}	0.536
d_{min}, Å	0.50
N_{meas}, N_{uniq}	267 745, 37 499
R_{int}	0.0573
R_{rim}, R_{pim}	0.0640, 0.0156
N_{obs}, N_{var}	27 748, 1982
$R(F)$, $R_w(F^2)$, all data	0.051, 0.037
goodness-of-fit	0.892
$\Delta\rho_{max}$, $\Delta\rho_{min}$ (e Å^{-3})	−0.25, 0.44

Table 2. Selected Geometrical Parameters for $[Co(SPh)_4]^{2-}$

bond	d (Å)	angle	degree (deg)
Co−S1	2.3273(2)	S1−Co−S2	112.8(1)
Co−S4	2.3254(2)	S1−Co−S3	96.6(1)
Co−S3	2.3327(2)	S1−Co−S4	116.2(1)
Co−S2	2.3132(2)	S2−Co−S3	119.9(1)
S1−C1	1.7630(8)	S2−Co−S4	98.6(1)
S2−C7	1.7658(10)	S3−Co−S4	113.9(1)
S3−C13	1.7588(9)		
S4−C19	1.7679(8)		

DOI: 10.1021/acs.inorgchem.8b00513
Inorg. Chem. 2018, 57, 6913−6920

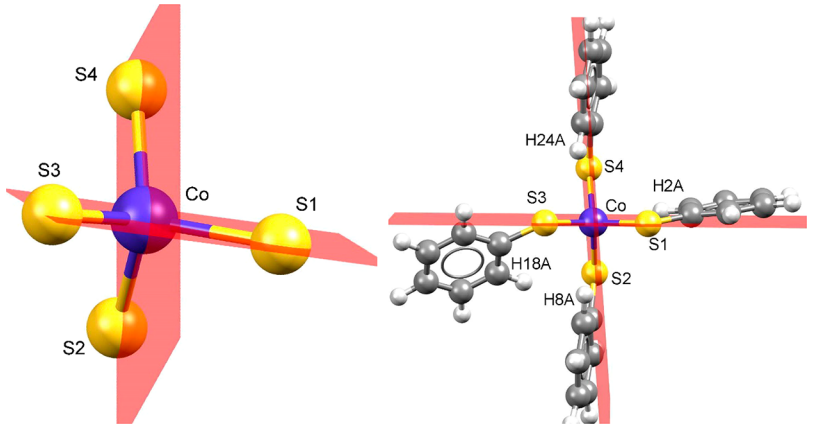

Figure 2. Definition of the two nearly perpendicular planes describing the first coordination sphere around the Co atom in the $[Co(SPh)_4]^{2-}$ complex.

metal site upon chemical bonding. To visualize the intricate effects of bonding, it is instructive to plot the static model deformation density, which is simply the difference between the modeled (and experimental) aspherical electron density and the unperturbed (and thus calculated) atomic densities. Such maps are shown in Figure 3 for four S−Co−S planes of the CoS_4 unit. Inspection around Co reveals that the regions of electronic depletion and accumulation (relative to neutral Co and S atoms) are asymmetrical with respect to the different bonds. The Co−S2 line passes directly through an electron depletion zone (indicated by red dashes) near Co, in contrast to the Co−S1 bond, which passes through a region where the deformation density is nearly zero. This difference is fully reflected in the location of the lone pair on the S atoms, which for all atoms face the depletion zones on Co.

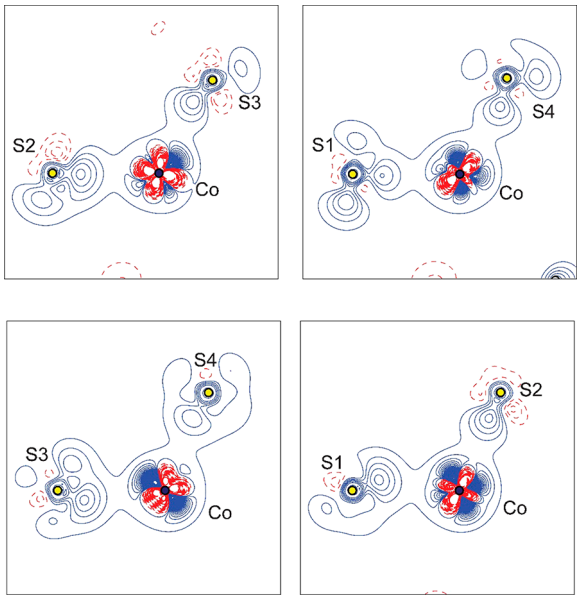

Figure 3. Deformation density in the different S−Co−S planes. Positive contours are shown with solid blue lines; negative contours are shown with dashed red lines. The contour interval is 0.1 e $Å^{-3}$.

The discrepancy in deformation densities for the Co−S bonds suggests varying degrees of covalency that are corroborated by the variation in bond distances of the four Co−S bonds (see Table 2) and the fact that the shortest bond (Co−S2) is the one that most directly faces a charge depletion region on Co. This latter observation is particularly relevant; because the detailed distribution of the valence electron density around Co (i.e., the pattern of charge depletion and accumulation regions) is a direct result of the d-orbital populations, it may be that the small but significant asymmetry in the Co−S bond distances is the determining factor for the splitting of the d orbitals.

The above-mentioned visual signs of asymmetry in the Co−S bonding are reflected in the topological analysis of the electron density (Table 3), where the Co−S2 bond is found to be markedly different from the other three Co−S bonds. This particular bond exhibits a slightly higher ρ_{bcp} value and a larger positive Laplacian ($\nabla^2\rho_{bcp}$) magnitude, which is in accordance with previous observations suggesting that a more positive value of $\nabla^2\rho_{bcp}$ accompanies an increase in bond strength.[48,49] This same trend is observed for the topological bond path, which is the unique line departing from the bond critical points toward the two atoms joined by these points, and along which the gradient of the density changes most rapidly. The length of the bond path for Co−S2 is nearly identical to the interatomic line, while significant deviations are seen for the other three

Table 3. Topological Parameters in the Co−S Bonds[a]

bond	d_{Co-S}	L_{BP}	Δd	ρ_{bcp}	$\nabla^2\rho_{bcp}$	V	H
Co−S1	2.3273(2)	2.3424	0.0151(0.6%)	0.45	5.92	−0.56	−0.07
Co−S2	2.3132(2)	2.3428	0.0043(0.2%)	0.48	6.19	−0.61	−0.09
Co−S3	2.3327(2)	2.3613	0.0286(1.2%)	0.44	5.98	−0.55	−0.07
Co−S4	2.3254(2)	2.3297	0.0296(1.3%)	0.44	5.76	−0.55	−0.07

[a]The Co−S distance, d_{Co-S}, the length of the bond path, L_{BP}, and the difference between the two, Δd, are given in angstroms, while the relative difference is given as a percentage. The value of ρ_{bcp} is given in e $Å^{-3}$, the Laplacian in e $Å^{-5}$, while the energy densities V and H are given in Hartree au^{-3}.

DOI: 10.1021/acs.inorgchem.8b00513
Inorg. Chem. 2018, 57, 6913−6920

bonds. Figure 4 shows the bond paths for the four Co−S bonds and clearly illustrates the linear behavior of the Co−S2 bond

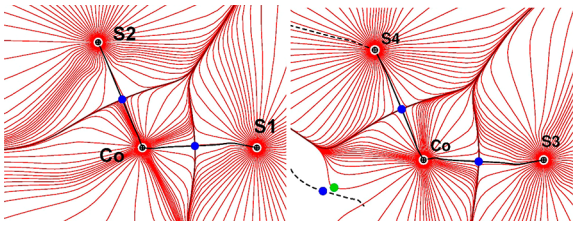

Figure 4. Electron density gradient trajectory plots in the plane of S1−Co−S2 (left) and S3−Co−S4 (right); the plots include 60 gradient paths starting from each nuclei. The blue circles indicate the bond critical points, and green circles are ring critical points, while the black lines show the bond paths.

path, in particular, while the bonds from Co to S1 and S3 are slightly bent.

The topological analysis also provides an estimate of the total energy densities in the bonds. All the values are negative, which suggests some degree of covalency in the bonds, and again the bond to S2 is set apart by its slightly larger values. As always, however, caution is required in the interpretation of these values due to the approximations made in their derivation.[26] A list of topological properties for all bonds is provided in the Supporting Information.

Before we address the d-orbital populations and hence the magnetic properties, it is relevant to first examine the atomic charges, as expressed by the integration over the zero-flux surface defined atomic basins (Table 4). First, the summed

Table 4. Atomic Charges Integrated over the Zero-Flux Surfaces

atom/group	Q
Co	+1.03
Co molecule	−1.37
cation1	+0.52
cation2	+0.92
⟨SPh groups⟩	−0.60

atomic charges for the three independent complex ions that make the neutral $(Ph_4P)_2[Co(SPh)_4]$ compound are −1.37, +0.52, and +0.92. Focusing on the magnetic complex, we find that Co has an atomic charge of +1.0 e, which is achieved without any electrons in the 4s shell, leading to a configuration that could be interpreted as $3d^8$. However, this integrated charge over the Co basin includes those electrons donated from dative bonds with the sulfur-based ligands.

DISCUSSION

Turning to the estimated d-orbital populations, which afford the most direct insight into the magnetic properties,[27,50] we emphasize that they should not to be interpreted as akin to any experimental observation of orbitals (which are not quantum mechanical observables) but merely result from the framework of the multipole model. This model employs spherical harmonics as its basis functions, which have a very clear correspondence to the angular functions used to describe the d-orbitals. In this analysis, we adhere to the local coordination system used in ref 11, which is defined such that the *z*-axis exactly bisects the S1−Co−S3 angle, and is thus parallel to the direction along which the first coordination sphere around Co is slightly elongated, constituting the approximate D_{2d} symmetry axis. The *x*-axis and *y*-axis are then chosen to align with the approximate C_2' rotation axes of the D_{2d} point group, such that the *x*-axis bisects the S1−Co−S4 angle, and the *y*-axis very nearly bisects the S1−Co−S2 angle, as shown in Figure 5.

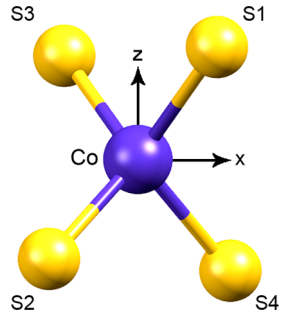

Figure 5. Illustration of the local coordinate system on Co. The view is down the *y*-axis.

The estimation of d-orbital populations from multipole parameters is associated with some uncertainty, as it is assumed that the full electron density described by the functions centered on the central Co belong to the metal atom. In other words, even if metal-based electron density results in part from ligand donation, it is treated here as having originated on the metal. Note that there are ways to obtain d-orbital populations from theoretical calculations, which deviate from the currently used procedure, for instance, by calculation of ab initio ligand field parameters.[51] However, we expect that all of these approaches should provide a coherent picture of the orbital populations without necessarily agreeing numerically, and we are currently exploring this issue in our research. The experimental d-orbital populations that result from the current approach are given in Table 5.

Table 5 also provides approximate theoretical d-orbital populations (in percentages of the total valence electron count), which were adapted directly from the d-orbital splitting diagram reported in ref 11 (also reproduced in Table 5). We note that, in the original publication, the two $m_l = \pm 2$ orbitals ($d_{x^2-y^2}$ and d_{xy}) are nearly degenerate, and the effect of this degeneracy would be to approximately equate the observed d-orbital populations. Indeed, this qualitative picture matches the results of our model, as the demonstrated distribution of charge at the cobalt atom arises from $d_{x^2-y^2}$ and d_{xy} orbitals that are nearly equally populated. The sum of the populations for these $m_l = \pm 2$ orbitals (39%) is close to that expected for 3/7 electrons (42.9%), with the model yielding a $d_{x^2-y^2}$ orbital slightly lower in energy than d_{xy}. The d_{z^2} orbital, which is lowest in energy from ref 6, is fully populated from our model (27.2%, ∼2/7 electrons = 28.6%). Finally, the two remaining d orbitals having $m_l = \pm 1$, d_{xz} and d_{yz}, possess populations of 15.8 and 18.1%, respectively, slightly above that expected for a 1/7 d electrons occupancy (14.3%). By scrutinizing the crystal structure in more detail, we can identify two plausible reasons why these two latter populations differ. First, the angle between the two planes defined by S1−Co−S3 and S2−Co−S4 deviates 3.7° from 90°, meaning that the *x*-axis and *y*-axis cannot be exactly identical relative to the sulfur atoms, and with the chosen axes, the *x*-axis points along the larger angle between Co−S bonds (see Figure 5). This positioning of the ligands

DOI: 10.1021/acs.inorgchem.8b00513
Inorg. Chem. 2018, 57, 6913−6920

Table 5. Experimental d-Orbital Populations Derived from the Refined Multipole Population Parameters and the Definition of the Local Coordinate Systems As Shown[a] in Figure 5

Orbital	Exp pop (%)	Theor pop (%)
d_{xz}	15.8	14.3
d_{yz}	18.1	14.3
d_{xy}	18.4	14.3
$d_{x^2-y^2}$	20.6	28.6
d_{z^2}	27.2	28.6

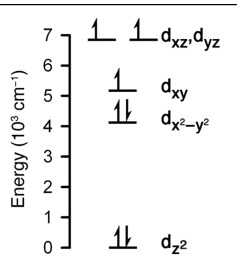

[a]With the *x*-axis and *y*-axis parallel to C_2' and *x* toward larger angles. To the far right is shown the original energy diagram and electron configuration for $(Ph_4P)_2[Co(SPh)_4]$ based on an angular overlap model as given in ref 11.

could potentially slightly destabilize the d_{yz} orbitals relative to the d_{xz}, although that contradicts the observed distribution, and thus if anything such destabilization is a minor effect.

An alternative explanation as to why the d_{xz} and d_{yz} populations differ may be that short interactions between Co and proximate H atoms influence the electron density of the former atom. Notably, there are four hydrogen atoms in close proximity to Co (H2A, H8A, H18A, and H24A from the phenyl rings attached to S1 to S4, respectively; see Figure 2b). Topological analysis of the electron density excludes the possibility that any of these hydrogen atoms participate in a Co−H chemical bond, as no bond critical points are found between them. Three of these H atoms experience relatively short Co···H separations (2.68 to 2.84 Å) and are also located near one of the two S−Co−S planes described previously (the distance to the closest plane is ∼0.4 Å; see Figure 2b). Because of their location near these planes, we do not anticipate that the hydrogen atoms interact appreciably with either the d_{xz} or d_{yz} orbitals, and therefore we do not expect these long-range Co···H interactions to contribute significantly to the observed difference in d_{xz}/d_{yz} populations. On the contrary, the fourth H atom, H18A, which is separated from Co by 3.105(1) Å, is oriented in the direction of both the $d_{x^2-y^2}$ and d_{xz} lobes, which suggests that this interaction may influence the energy of both these orbitals. An appreciable interaction will lift the degeneracy of the d_{xz}/d_{yz} pair, increasing the energy of the d_{xz} orbital and consequently lowering its population. Indeed, this observation is supported by the d_{xz}/d_{yz} orbital populations given in Table 5. Similarly, the location of H18A would increase the energy of the $d_{x^2-y^2}$ orbital, such that d_{xy} and $d_{x^2-y^2}$ would approach degeneracy, which is also confirmed in the experimental populations in Table 5.

The deformation density in the *xy* plane is illustrated in Figure 6 and clearly shows anisotropy in the electron density around Co arising from an uneven occupation of relevant d-orbitals. Three negative regions can be seen in the figure, but the fourth, approximately along the negative *y*-axis, is limited to a very small region close to the nucleus. If all four negative regions had been of equal size this would resemble what is found for a $(d_{x^2-y^2})^2(d_{xy})^1$ configuration. However, in addition to the near absence of the fourth region of negative deformation density, the three negative lobes near Co are not exactly perpendicular, suggesting that the electron density near Co does not originate purely from d-orbitals.

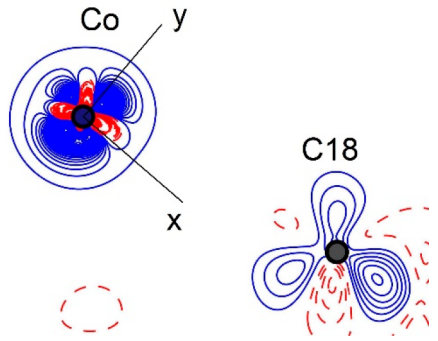

Figure 6. Deformation density in the *xy*-plane near Co. Positive contours are shown with blue solid lines, and negative contours are shown with red dashed lines. The contour interval is 0.1 e Å^{-3}.

CONCLUSIONS

The foregoing results highlight the utility of applying electron density studies to elucidate the electronic structure of metal ions and, specifically, the potential influence of longer-range interatomic interactions. The experimental electron density for the single-molecule magnet $[Co(SPh)_4]^{2-}$ corroborates the partly covalent nature of the Co−S bonds as previously suggested by spectroscopic analysis.[7] The estimated d-orbital populations distinguish the lower-lying, fully occupied d_{z^2} orbital from the pair of d_{xy} and $d_{x^2-y^2}$ orbitals, of which the latter is slightly more populated. This distribution of d electrons is notably influenced by the presence of one hydrogen atom located at a distance of 3.1 Å from Co, belonging to the only phenyl ring significantly tilted with respect to the two perpendicular S−Co−S planes defining the approximate D_{2d} point-group symmetry. This H atom exerts an electrostatic influence on the electronic structure of the Co atom without engaging in chemical bonding to the extent that would be visible by the presence of a topological bond critical point. One extremely important effect of this interaction is an increase in energy of both the $d_{x^2-y^2}$ and d_{xz} orbitals, such that $d_{x^2-y^2}$ and d_{xy} become nearly degenerate and thus equally populated, while the energy of d_{xz} is increased above that of d_{yz}). We are currently exploring means for altering the position of this H atom to confirm its influence on the electronic (and thus magnetic) properties of the $[Co(SPh)_4]^{2-}$ complex. For example, application of external pressure would modify the torsion angles within the molecular unit, while deuteration would have a smaller but perhaps appreciable influence as well. Investigation of the $[Co(OPh)_4]^{2-}$ anion using the approach detailed here may also be of interest to identify whether a stronger ligand field, completely devoid of any π-activity, would translate into an increased splitting of the $d_{x^2-y^2}$, d_{xy}, and d_{xz} orbitals at intermediate energies.

DOI: 10.1021/acs.inorgchem.8b00513
Inorg. Chem. 2018, 57, 6913−6920

■ ASSOCIATED CONTENT

Supporting Information

The Supporting Information is available free of charge on the ACS Publications website at DOI: 10.1021/acs.inorgchem.8b00513.

X-ray crystallography data reduction and model refinement, local coordinate system, atomic displacement parameters, anharmonicity, spatial Laplacian distribution, residual density analysis, normal probability plots, topological analysis (PDF)

Accession Codes

CCDC 1829296 contains the supplementary crystallographic data for this paper. These data can be obtained free of charge via www.ccdc.cam.ac.uk/data_request/cif, or by emailing data_request@ccdc.cam.ac.uk, or by contacting The Cambridge Crystallographic Data Centre, 12 Union Road, Cambridge CB2 1EZ, UK; fax: +44 1223 336033.

■ AUTHOR INFORMATION

Corresponding Author

*E-mail: jacobo@chem.au.dk.

ORCID

Joseph M. Zadrozny: 0000-0002-1309-6545

Jeffrey R. Long: 0000-0002-5324-1321

Jacob Overgaard: 0000-0001-6492-7962

Present Address

⊥J.M.Z. Department of Chemistry, Colorado State University, Ft. Collins, CO 80523, United States.

Author Contributions

The manuscript was written through contributions of all authors. All authors have given approval to the final version of the manuscript.

Funding

Danish National Research Foundation; U.S. National Science Foundation

Notes

The authors declare no competing financial interest.

■ ACKNOWLEDGMENTS

The authors thank the Danish National Research Foundation for financial support (DNRF-93). J.R.L. and J.M.Z. acknowledge support from the U.S. National Science Foundation under Grant No. CHE-1464841.

■ REFERENCES

(1) Leuenberger, M. N.; Loss, D. Quantum computing in molecular magnets. *Nature* **2001**, *410* (6830), 789−793.

(2) McInnes, E. J. L.; Timco, G. A.; Whitehead, G. F. S.; Winpenny, R. E. P. Heterometallic Rings: Their Physics and use as Supramolecular Building Blocks. *Angew. Chem., Int. Ed.* **2015**, *54* (48), 14244−14269.

(3) Sessoli, R.; Gatteschi, D.; Caneschi, A.; Novak, M. A. Magnetic Bistability in a Metal-Ion Cluster. *Nature* **1993**, *365* (6442), 141−143.

(4) Ako, A. M.; Hewitt, I. J.; Mereacre, V.; Clérac, R.; Wernsdorfer, W.; Anson, C. E.; Powell, A. K. A Ferromagnetically Coupled Mn19 Aggregate with a Record S = 83/2 Ground Spin State. *Angew. Chem., Int. Ed.* **2006**, *45* (30), 4926−4929.

(5) Ishikawa, N.; Sugita, M.; Ishikawa, T.; Koshihara, S.; Kaizu, Y. Lanthanide double-decker complexes functioning as magnets at the single-molecular level. *J. Am. Chem. Soc.* **2003**, *125* (29), 8694−8695.

(6) Bar, A. K.; Pichon, C.; Sutter, J.-P. Magnetic anisotropy in two- to eight-coordinated transition−metal complexes: Recent developments in molecular magnetism. *Coord. Chem. Rev.* **2016**, *308*, 346−380.

(7) Frost, J. M.; Harriman, K. L. M.; Murugesu, M. The rise of 3-d single-ion magnets in molecular magnetism: towards materials from molecules? *Chem. Sci.* **2016**, *7* (4), 2470−2491.

(8) Gómez-Coca, S.; Aravena, D.; Morales, R.; Ruiz, E. Large magnetic anisotropy in mononuclear metal complexes. *Coord. Chem. Rev.* **2015**, *289−290*, 379−392.

(9) Craig, G. A.; Murrie, M. 3d single-ion magnets. *Chem. Soc. Rev.* **2015**, *44* (8), 2135−2147.

(10) Atanasov, M.; Aravena, D.; Suturina, E.; Bill, E.; Maganas, D.; Neese, F. First principles approach to the electronic structure, magnetic anisotropy and spin relaxation in mononuclear 3d-transition metal single molecule magnets. *Coord. Chem. Rev.* **2015**, *289−290*, 177−214.

(11) Zadrozny, J. M.; Long, J. R. Slow Magnetic Relaxation at Zero Field in the Tetrahedral Complex [Co(SPh)4]2−. *J. Am. Chem. Soc.* **2011**, *133* (51), 20732−20734.

(12) Zadrozny, J. M.; Telser, J.; Long, J. R. Slow magnetic relaxation in the tetrahedral cobalt(II) complexes [Co(EPh)4]2− (EO, S, Se). *Polyhedron* **2013**, *64* (0), 209−217.

(13) Suturina, E. A.; Nehrkorn, J.; Zadrozny, J. M.; Liu, J.; Atanasov, M.; Weyhermüller, T.; Maganas, D.; Hill, S.; Schnegg, A.; Bill, E.; Long, J. R.; Neese, F. Magneto-Structural Correlations in Pseudotetrahedral Forms of the [Co(SPh)4]2− Complex Probed by Magnetometry, MCD Spectroscopy, Advanced EPR Techniques, and ab Initio Electronic Structure Calculations. *Inorg. Chem.* **2017**, *56* (5), 3102−3118.

(14) Suturina, E. A.; Maganas, D.; Bill, E.; Atanasov, M.; Neese, F. Magneto-Structural Correlations in a Series of Pseudotetrahedral [CoII(XR)4]2− Single Molecule Magnets: An ab Initio Ligand Field Study. *Inorg. Chem.* **2015**, *54* (20), 9948−9961.

(15) Coste, S. C.; Vlaisavljevich, B.; Freedman, D. E. Magnetic Anisotropy from Main-Group Elements: Halides versus Group 14 Elements. *Inorg. Chem.* **2017**, *56* (14), 8195−8202.

(16) Dance, I. G. Synthesis, crystal structure, and properties of the hexa(.mu.-benzenethiolato)tetra(benzenethiolatocobaltate(II)) dianion, the prototype cobalt(II)-thiolate molecular cluster. *J. Am. Chem. Soc.* **1979**, *101* (21), 6264−6273.

(17) Swenson, D.; Baenziger, N. C.; Coucouvanis, D. Tetrahedral Mercaptide complexes. Crystal and Molecular Structures of $[(C_6H_5)_4P]_2M(SC_6H_5)_4$ Complexes (M = Cd(II), Zn(II), Co(II), and Mn(II)). *J. Am. Chem. Soc.* **1978**, *100*, 1932.

(18) Holah, D. G.; Coucouvanis, D. Synthesis and characterization of a new series of first row element tetrahedral mercaptide complexes. *J. Am. Chem. Soc.* **1975**, *97*, 6917.

(19) Coucouvanis, D.; Swenson, D.; Baenziger, N. C.; Murphy, C.; Holah, D. G.; Sfarnas, N.; Simopoulos, A.; Kostikas, A. Tetrahedral complexes containing the Fe(II)S4 core. The syntheses, ground-state electronic structures and crystal and molecular structures of the bis(tetraphenylphosphonium) tetrakis (thiophenolato)ferrate (II) and bis (tetrapheny lphosphonium) bis(dithiosquarato)ferrate (II) complexes. An analog for the active site in reducd rubredoxins (Rdred). *J. Am. Chem. Soc.* **1981**, *103* (12), 3350−3362.

(20) Coppens, P. *X-Ray Charge Densities and Chemical Bonding (International Union of Crystallography Texts on Crystallography)*; International Union of Crystallography, 1997; p 384.

(21) Overgaard, J. *Applications of electron density studies in molecular and solid-state science*. Ph.D. Dissertation. Faculty of Science and Technology, Aarhus University, 2015; p 390.

(22) Jorgensen, M. R. V.; Hathwar, V. R.; Bindzus, N.; Wahlberg, N.; Chen, Y.-S.; Overgaard, J.; Iversen, B. B. Contemporary X-ray electron-density studies using synchrotron radiation. *IUCrJ* **2014**, *1* (5), 267−280.

(23) Stalke, D., Charge Density and Chemical Bonding. In *The Chemical Bond I: 100 Years Old and Getting Stronger*; Mingos, D. M. P., Ed.; Springer International Publishing: Cham, Switzerland, 2016; pp 57−88.

DOI: 10.1021/acs.inorgchem.8b00513
Inorg. Chem. 2018, 57, 6913−6920

(24) Stalke, D. Meaningful Structural Descriptors from Charge Density. *Chem. - Eur. J.* **2011**, *17* (34), 9264−9278.
(25) Gatti, C.; Macchi, P. *Modern Charge-Density Analysis,* 1st ed.; Springer: Dordrecht, Netherlands, 2012; p xxiii + 783.
(26) Gatti, C. Chemical bonding in crystals: new directions. *Z. Kristallogr. - Cryst. Mater.* **2005**, *220* (5−6), 399−457.
(27) Holladay, A.; Leung, P.; Coppens, P. Generalized Relations between D-Orbital Occupancies of Transition-Metal Atoms and Electron-Density Multipole Population Parameters from X-Ray-Diffraction Data. *Acta Crystallogr., Sect. A: Found. Crystallogr.* **1983**, *39* (May), 377−387.
(28) Macchi, P.; Sironi, A. Chemical bonding in transition metal carbonyl clusters: complementary analysis of theoretical and experimental electron densities. *Coord. Chem. Rev.* **2003**, *238*, 383−412.
(29) Bader, R. F. W. *Atoms In Molecules;* Oxford University Press, 1990.
(30) Abramov, Y. A. On the possibility of kinetic energy density evaluation from the experimental electron-density distribution. *Acta Crystallogr., Sect. A: Found. Crystallogr.* **1997**, *53*, 264−272.
(31) Kirshnitz, D. A. Quantum Corrections to the Thomas-Fermi Equation. *JETP* **1957**, *5*, 64.
(32) *CrysAlisPRO;* Agilent Technologies UK Ltd: Yarnton, England, 2013.
(33) Blessing, R. H. Data Reduction and Error Analysis for Accurate Single Crystal Diffraction Intensities. *Crystallogr. Rev.* **1987**, *1* (1), 3−58.
(34) Sheldrick, G. SHELXT - Integrated space-group and crystal-structure determination. *Acta Crystallogr., Sect. A: Found. Adv.* **2015**, *71* (1), 3−8.
(35) Sheldrick, G. Crystal structure refinement with SHELXL. *Acta Crystallogr., Sect. C: Struct. Chem.* **2015**, *71* (1), 3−8.
(36) Dolomanov, O. V.; Bourhis, L. J.; Gildea, R. J.; Howard, J. A. K.; Puschmann, H. OLEX2: a complete structure solution, refinement and analysis program. *J. Appl. Crystallogr.* **2009**, *42*, 339−341.
(37) Johnson, C. K. *ORTEP;* Oak Ridge National Laboratory: Tennessee, 1965.
(38) Hansen, N. K.; Coppens, P. Electron Population Analysis of Accurate Diffraction Data 0.6. Testing Aspherical Atom Refinements on Small-Molecule Data Sets. *Acta Crystallogr., Sect. A: Cryst. Phys., Diffr., Theor. Gen. Crystallogr.* **1978**, *34* (Nov), 909−921.
(39) Volkov, A.; Macchi, P.; Farrugia, L. J.; Gatti, C.; Mallinson, P.; Richter, T.; Koritsanszky, T. *XD2006, A Computer Program Package for Multipole Refinement, Topological Analysis of Charge Densities and Evaluation of Intermolecular Energies from Experimental and Theoretical Structure Factors;* University of Glasgow, 2006. Online at http://xd.chem.buffalo.edu/.
(40) Allen, F. H.; Kennard, O.; Watson, D. G.; Brammer, L.; Orpen, A. G.; Taylor, R. Tables of bond lengths determined by X-ray and neutron diffraction. Part 1. Bond lengths in organic compounds. *J. Chem. Soc., Perkin Trans. 2* **1987**, No. 12, S1−S19.
(41) Macchi, P.; Coppens, P. Relativistic analytical wave functions and scattering factors for neutral atoms beyond Kr and for all chemically important ions up to I-. *Acta Crystallogr., Sect. A: Found. Crystallogr.* **2001**, *57*, 656−662.
(42) Su, Z. W.; Coppens, P. Nonlinear least-squares fitting of numerical relativistic atomic wave functions by a linear combination of Slater-type functions for atoms with Z = 1−36. *Acta Crystallogr., Sect. A: Found. Crystallogr.* **1998**, *54*, 646−652.
(43) Herbst-Irmer, R.; Henn, J.; Holstein, J. J.; Hübschle, C. B.; Dittrich, B.; Stern, D.; Kratzert, D.; Stalke, D. Anharmonic Motion in Experimental Charge Density Investigations. *J. Phys. Chem. A* **2013**, *117* (3), 633−641.
(44) Hirshfeld, F. L. Can X-Ray Data Distinguish Bonding Effects from Vibrational Smearing. *Acta Crystallogr., Sect. A: Cryst. Phys., Diffr., Theor. Gen. Crystallogr.* **1976**, *32* (Mar1), 239−244.
(45) Henn, J.; Meindl, K. About systematic errors in charge-density studies. *Acta Crystallogr., Sect. A: Found. Adv.* **2014**, *70*, 248−256.
(46) Meindl, K.; Henn, J.; Stalke, D. Residual Density Analysis. *Struct. Bonding* **2010**, *147*, 143−192.
(47) Pinsky, M.; Avnir, D. Continuous Symmetry Measures. 5. The Classical Polyhedra. *Inorg. Chem.* **1998**, *37* (21), 5575−5582.
(48) Overgaard, J.; Hibbs, D. E.; Rentschler, E.; Timco, G. A.; Larsen, F. K. Experimental and theoretical electron density distribution and magnetic properties of the butterfly-like complex [Fe(4)O(2)(O(2)-CCMe(3))(8)(NC(5)H(4)Me)(2)].2CH(3)CN. *Inorg. Chem.* **2003**, *42* (23), 7593−601.
(49) Gibbs, G. V.; Downs, R. T.; Cox, D. F.; Rosso, K. M.; Ross, N. L.; Kirfel, A.; Lippmann, T.; Morgenroth, W.; Crawford, T. D. Experimental bond critical point and local energy density properties determined for Mn-O, Fe-O, and Co-O bonded interactions for tephroite, Mn2SiO4, fayalite, Fe2SiO4, and Co2SiO4 olivine and selected organic metal complexes: Comparison with properties calculated for non-transition and transition metal M-O bonded interactions for silicates and oxides. *J. Phys. Chem. A* **2008**, *112* (37), 8811−8823.
(50) Sabino, J. R.; Coppens, P. On the choice of d-orbital coordinate system in charge-density studies of low-symmetry transition-metal complexes. *Acta Crystallogr., Sect. A: Found. Crystallogr.* **2003**, *59* (2), 127−131.
(51) Atanasov, M.; Zadrozny, J. M.; Long, J. R.; Neese, F. A theoretical analysis of chemical bonding, vibronic coupling, and magnetic anisotropy in linear iron(ii) complexes with single-molecule magnet behavior. *Chem. Sci.* **2013**, *4* (1), 139−156.

DOI: 10.1021/acs.inorgchem.8b00513
Inorg. Chem. 2018, 57, 6913−6920